Published in "Physical Review E 90(6): 060301, 2014"
which should be cited to refer to this work.

Accounting for inertia effects to access the high-frequency microrheology of viscoelastic fluids

P. Domínguez-García,[1,*] Frédéric Cardinaux,[2,3] Elena Bertseva,[4] László Forró,[4] Frank Scheffold,[2] and Sylvia Jeney[4]

[1]*Departamento de Física de Materiales, Universidad Nacional de Educación a Distancia (UNED), Madrid 28040, Spain*

[2]*Department of Physics, University of Fribourg, 1700 Fribourg Perolles, Switzerland*

[3]*LS Instruments AG, Passage du Cardinal 1, CH-1700 Fribourg, Switzerland*

[4]*Laboratory of Physics of Complex Matter, Ecole Polytechnique Fédérale de Lausanne (EPFL), 1015 Lausanne, Switzerland*

We study the Brownian motion of microbeads immersed in water and in a viscoelastic wormlike micelles solution by optical trapping interferometry and diffusing wave spectroscopy. Through the mean-square displacement obtained from both techniques, we deduce the mechanical properties of the fluids at high frequencies by explicitly accounting for inertia effects of the particle and the surrounding fluid at short time scales. For wormlike micelle solutions, we recover the 3/4 scaling exponent for the loss modulus over two decades in frequency as predicted by the theory for semiflexible polymers.

e quantitative stochastic description of Brownian motion [1] of spherical micro- and nanobeads in complex fluids has laid the foundation for the invention of *tracer microrheology* [2,3], a powerful, noninvasive method that allows the measurement of mechanical properties over an extended range of frequencies using all optical instrumentation. At very short time scales, or high frequencies, the stochastic description of Brownian motion fails as pointed out already in the original work of Einstein [4]. At microsecond time scales the influence of inertial effects and hydrodynamic memory becomes sizable [5,6]. Failing to account for these contributions leads to substantial errors. Removing these effects [7,8] at high frequencies ω when calculating the complex modulus, $G^*(\omega)$, may allow one to discern relevant data that is otherwise difficult or impossible to access. Elastic moduli at such high frequencies may contain important information about living cells [9], biopolymers in pharmaceutical applications [10], or fast processes encountered, for example, in ink-jet printing [11].

In this work, we demonstrate how to correct for the influence of inertia in an actual experiment. We study the Brownian motion of microbeads immersed in water and in a viscoelastic wormlike micelle solution by two complementary experimental techniques accessing the MHz frequency range: optical trapping microscopy (OTI) and diffusing wave spectroscopy (DWS). The combined application of these two methods is unique since it covers the most relevant approaches to high-frequency microrheology, while other methods, such as particle tracking, are limited to frequencies well below 10 kHz [12]. We account for inertia effects quantitatively using two different approaches: the self-consistent correction of the mean-square displacement suggested in Ref. [13] and a theoretical expression derived from the recent work of Schieber and collaborators [14,15]. We find that these two different quantitative methods provide similar results, as shown by a study of the high-frequency scaling of the modulus $G''(\omega) \sim \omega^{\alpha}$ of a viscoelastic wormlike micelle solution. Taking into account inertia effects we find an exponent of $\alpha \cong 0.75$, as predicted by the theory for semiflexible polymers [16]. Besides, the proposed methodology allows one to extract parameters relevant to the intrinsic properties of the viscoelastic fluid, such as the bending modulus, the mesh size, and the contour length of the molecular components.

In a tracer microrheology experiment, the complex modulus of a bulk material is calculated from the measured mean-square displacements [MSD $\equiv \langle[\mathbf{r}(t) - \mathbf{r}(0)]^2\rangle$] of microbeads with position $\mathbf{r}(t)$ [2,17]. OTI is the more versatile of the two techniques as it acts on individual beads and, therefore, does not rely on averaging over the motion of many beads, as is the case for DWS. In OTI, the movement of a single microbead is recorded by means of an interferometric position detector [18]. The bead is trapped in the center of a sample chamber using optical tweezers [19], applying the lowest optical force available, $3 \lesssim k \lesssim 10$ μN/m, where k is the spring constant of the optical restoring force. DWS is an extension of dynamic light scattering applied to materials with strong multiple scattering [12,20–22] and it allows precise measurements of the three-dimensional movement of tracer beads in the complex fluid. The advantages of DWS are its relative ease of use employing standard spectrophotometer cuvettes and the minute-scale measurement times with little calibration and postprocessing required. DWS also provides access to a large range of experimental parameters and can be applied to viscoelastic fluids and solids with low- or high-frequency moduli while covering an extended range of frequencies from $\omega \sim 0.1$ to 10^6 rad/s [13]. By directly comparing the results obtained by each of the techniques, we study the Brownian motion of melamine resin microbeads with radii $a = 0.94$ or 1.47 μm, with density $\rho_p = 1570$ kg/m^3 at $T = 21\,^{\circ}$C. The relatively high refractive index ($n = 1.68$) provides good trapping efficiency in OTI experiments. It has been reported in Ref. [23] that the colloid surface chemistry of the microbeads can affect the results obtained by microrheology. Such effects are particularly relevant for protein specific bonding in biomaterials. In our case, however, the resin beads are chemically nonactive and therefore we expect such effects to be negligible. The sample under study is an aqueous solution at 4 wt% of surfactant cetylpyridinium chloride (CPy^+Cl^-) and sodium salicylate (Na^+Sal^-) that self-assemble into a wormlike micelle solution [24]. At sufficiently high frequencies the cylindrical micelles are

*pdominguez@fisfun.uned.es

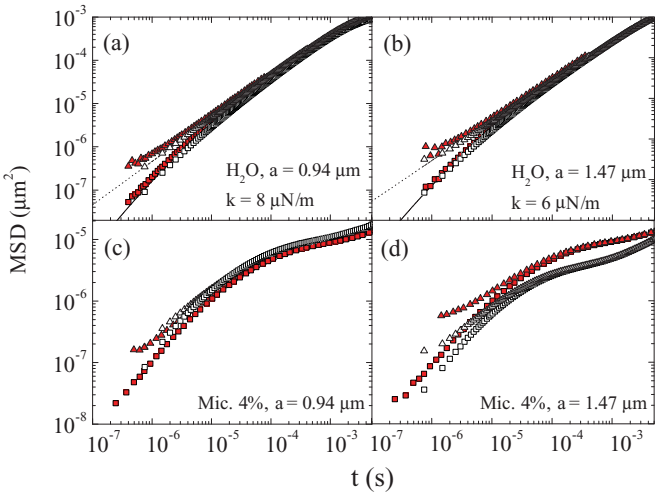

FIG. 1. (Color online) One-dimensional particle MSD in water and in a 4% micellar solution for two different bead sizes a. Experimental data: OTI (□) and DWS (■). Corrected MSDs are shown as triangles: from OTI (△) and from DWS (▲). Theoretical predictions for water: Chandrasekhar's result ignoring inertia effects (- - -) and Hinch's prediction including the influence of inertia (——).

expected to behave as a solution of semiflexible polymers in the semidilute regime formed by entangled micelles [25]. We measure the steady-state viscosity using a Rheometer MCR502 (Anton Paar, Austria) at 21 °C, which yields to $\eta_0 = 360$ mPa s. In the OTI experiments, a double flow chamber is used: One of the chambers contains water and beads at very low concentration, while the other one encloses the viscoelastic fluid with the same type of beads. After aligning the optical trapping light path to the position detector and adjusting signal amplification, a calibration experiment is performed in the pure water solution. The measurement in the viscoelastic solution is done right afterwards. This procedure allows using the known properties of a Newtonian fluid [26] to extract the volts-to-meter conversion factor β, which is then used to calculate the MSD in the viscoelastic medium [27]. For the DWS experiments, we are using a bead concentration of 2 vol%. Samples are loaded into standard rectangular spectrometer cuvettes with a path length $L =$ 2 mm or $L = 5$ mm and a width of 10 mm. Echo two-cell DWS experiments in transmission geometry are performed as described in Ref. [28]. The two experimental techniques provide similar MSDs for the bead motion in water, as shown in Figs. 1(a) and 1(b). However, for the micelle solution, some differences are observed Figs. 1(c) and 1(d), in particular for the larger bead size. Similar global shifts of the MSD have been observed previously [29,30]. They have been attributed to hydrodynamic effects at the fluid-particle interface and local perturbations of the equilibrium configuration of the complex fluid [31]. The optical force in a micelle solution might trap some of the polymeric structure, hindering the Brownian motion and, thereby, slightly incrementing the apparent measured viscosity of the fluid. DWS in turn is sensitive to depletion of the surfactant solution around the beads and a possible onset of depletion-induced bead attraction which can result in enhanced motion and larger MSD values [30]. To observe the effects of inertia and hydrodynamics in the MSDs, we compare in Figs. 1(a) and 1(b) the results obtained for bead motion in pure water with the Chandrasekhar expression for a classic Newtonian fluid [32], given by $\langle \Delta r^2(t) \rangle = [1 - \exp(-kt/\gamma)]\, 2k_B T/k$ where $\gamma = 6\pi\eta a$. For the case of DWS, there is no optical trap and the classical Stokes-Einstein result $\langle \Delta r^2(t) \rangle = (k_B T/3\pi\eta a)\, t$ is recovered in the limit $k \to 0$. In both cases, substantial deviations due to inertial effects are observed at times shorter than $t = 10^{-4}$ s. For water, the inertia effects in the MSD can be reproduced quantitatively using the classical result according to Hinch [33] Figs. 1(a) and 1(b).

The standard formalism to convert the measured MSD to the complex elastic modulus $G^*(\omega)$ is the Mason-Weitz (MW) approach based on the generalized Stokes-Einstein relation (GSER) [22] concurrent with Mason's approximation [34] to obtain

$$Z^*(\omega) = \frac{k_B T}{i\omega\pi a \overline{\langle \Delta r^2(\omega) \rangle}}, \tag{1}$$

where $\overline{\langle \Delta r^2(\omega) \rangle}$ is the one-side Fourier transform of the MSD. In the absence of inertia effects, $G^*(\omega) \equiv Z^*(\omega)$ for equilibrium Brownian motion in a homogeneous viscoelastic fluid [17]. An alternative methodology to connect the MSDs with the rheological properties of the fluid was reported by Evans *et al.* [35]. Both methods [36] have common limitations, such as the omission of optical or external forces, the neglect particle and fluid inertia, and the nonconsideration of active and heterogeneous materials [37]. The inertia effects appearing in the power-spectral density (PSD) of probe particles using optical tweezers were studied in Refs. [38,39], while a systematic approach to account for inertia effects in the MSD obtained from passive bead microrheology has been described in Ref. [13]. The principal idea in the latter work is to define an effective viscosity of the medium by $\eta_{\rm eff}(t) = [k_B T/3\pi \langle \Delta r^2(t) \rangle a]\, t$ and then calculate, for each measured time point t, the correction factor $f(t, \eta_{\rm eff}(t)) \geqslant 1$ for the MSD using the known theoretical result for a Newtonian fluid [33]. The procedure is iterated numerically starting with the measured MSD. The MSD obtained after correction is used for further processing in Eq. (1). The same strategy has been applied in Ref. [40] using the PSD [41]. A more fundamental theoretical treatment has been suggested by Felderhof [42] and more recently by Indei *et al.* [14] and Córdoba *et al.* [15]. The latter work conveniently provides an analytical expression relating the actual complex modulus and the bead mean-square displacement, assuming that the medium is incompressible [43]:

$$G^*(\omega) = Z^*(\omega) + \frac{m^*\omega^2}{6\pi a} + \frac{a^2\omega^2}{2} \times \left[\sqrt{\rho^2 - \frac{2\rho}{3\pi a^3} \left(\frac{6\pi a}{\omega^2} Z^*(\omega) + m^* \right)} - \rho \right], \tag{2}$$

where $m^* = m_{\rm particle} + 2\pi\rho a^3/3$ is the effective mass of the particle. By calculating $Z^*(\omega)$ and then using Eq. (2), we obtain the complex moduli without the influence of inertia. It is important to note that other possible corrections to the high-frequency bead motion, for example due deviations from

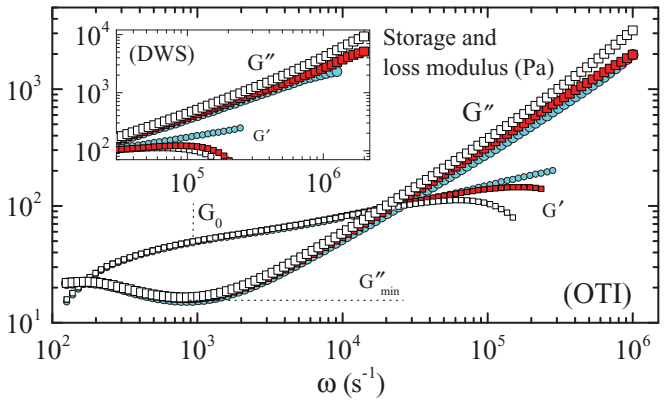

FIG. 2. (Color online) Comparison of the microrheology results using OTI and DWS (inset) for one bead size $a = 0.94\ \mu$m in a viscoelastic micelle solution with and without taking into account the effects of inertia. Data without inertia correction (□), corrected using Eq. (2) (■), and using the corrected MSDs shown in Fig. 1 (●).

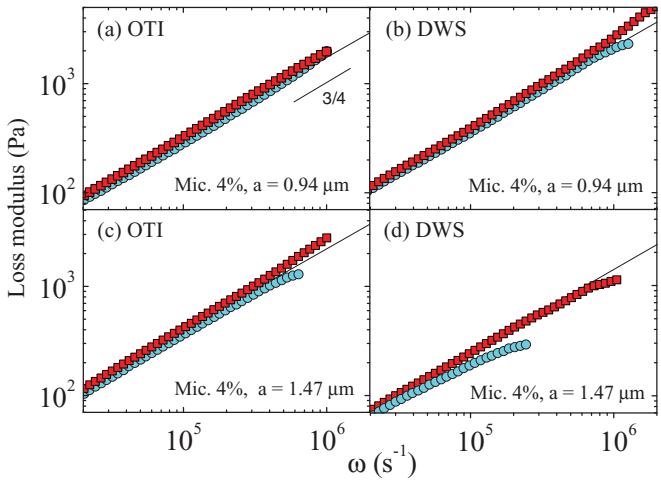

FIG. 3. (Color online) High-frequency loss modulus $G''(\omega) - \omega\eta_s$ compared to theoretical predictions. Inertia-corrected data using Eq. (2) (■) and using the corrected MSDs shown in Fig. 1 (●). (a) OTI, $a = 0.94\ \mu$m. (b) DWS, $a = 0.94\ \mu$m. (c) OTI, $a = 1.47\ \mu$m. (d) DWS, $a = 1.47\ \mu$m. Black line (——) is $G''_{\rm GMK}(\omega) - \omega\eta_s$ evaluated using Eq. (3) and data from Table I.

the GSER at $\omega \geqslant 10^6$ Hz, are not included by these corrections [17].

We apply these correction protocols to the experimental MSDs displayed in Fig. 1 to obtain the complex modulus for the micelle solution. In Fig. 2 we show the results derived from DWS and OTI using a bead size $a = 0.94\ \mu$m [44] for OTI and DWS, with and without corrections. The inertia-corrected results for $G''(\omega)$ calculated using both methods yield to similar results. These results can be compared to the the expected behavior at higher frequencies for a solution of semiflexible polymers, which, according to Gittes and MacKintosh [16], is given by

$$G^*_{\rm GMK}(\omega) = i\omega\eta_s + \frac{1}{15}\rho_m \kappa l_p \left(\frac{-2i\xi}{\kappa}\right)^{3/4} \omega^{3/4}. \quad (3)$$

Then, it is expected that both moduli, loss and storage, follow the $G^* \sim \omega^{3/4}$ behavior at high frequencies. However, at high frequencies the viscous response of the material dominates the elastic response by about an order of magnitude. This makes it very difficult to extract meaningful information about G' from microrheology. We thus restrict our discussion to the comparison of Eq. (2) using only the experimental loss modulus, G'', for CpyCl/NaSal to study in more detail the accuracy of inertia corrections at high frequencies [45]. Next, we compare Eq. (3) using only the experimental loss modulus for CpyCl/NaSal to study in more detail the accuracy of inertia corrections at high frequencies. To evaluate Eq. (3), we use the standard theory of polymers [46] and the experimental G_0, $G''_{\rm min}$, and ω_0 as input parameters. The quantity G_0 is the value of G' at which G'' has a local minimum, denoted as $G''_{\rm min}$. Both characteristic values can be easily obtained from Fig. 2. The third input parameter is ω_0, the crossover frequency where the exponent α of the power-law behavior $G'' \sim \omega^\alpha$ changes from the Rouse-Zimm behavior to the expected 3/4 at higher frequencies [47]. The persistence length of the polymerlike micelles is then linked to ω_0 by $l_p = (kT/8\eta_s\omega_0)^{1/3}$. The micelles diameter is estimated as $d_{\rm mic} = 2.5$ nm [13] and the area density is $\rho_m = \phi/[(\pi/4)d^2_{\rm mic}] = 8.2 \times 10^{15}$ m^{-2}, where ϕ is the volumetric concentration [30]. Then, we calculate the bending modulus, $\kappa = kT\,l_p$, the mesh size, $\xi = (kT/G_0)^{1/3}$, the lateral drag coefficient, $\zeta = 4\pi\eta_s/\ln(0.6\lambda/d_{\rm mic})$ where $\lambda = \xi$, the contour length between two entanglements, $l_e = \xi^{5/3}/lp^{2/3}$, and the contour length of the micelles, $L = l_e\,G_0/G''_{\rm min}$. The results of the calculations for these quantities are summarized in Table I. The different experimental methods (DWS and OTI) as well as the two bead sizes give similar results. The averaged persistence length, $l_p \sim 33 \pm 6$ nm, agrees with previous mechanical measurements for this kind of surfactant solution (29 nm) [13], but the averaged mesh size, $\xi \sim 42$ nm, is slightly lower (52 nm). To quantify the inertia corrections for the viscoelastic fluid at frequencies 10^4–10^6 Hz, we plot in Fig. 3 the loss modulus obtained from applying the two different correction procedures. The results quantitatively agree with theory, except for some deviations due to the limited accuracy of the

TABLE I. Characteristic magnitudes for the wormlike micelle solution obtained from OTI and DWS using Eq. (3). For all data $d_{\rm mic} = 2.5$ nm and area density $\rho_m = 8.2 \times 10^{15}$ m^{-2}.

a (μm)	Tech.	ω_0 (s^{-1} $\times 10^4$)	G_0 (Pa)	$G''_{\rm min}$ (Pa)	l_p (nm)	κ (J m $\times 10^{-29}$)	ξ (nm)	ζ (Ns/m^2 $\times 10^{-3}$)	l_e (nm)	L (nm)
0.94	OTI	1.7 ± 0.1	50 ± 5	15 ± 2	31.0 ± 0.6	12.6 ± 0.3	43 ± 1	5.4 ± 0.2	54 ± 4	180 ± 50
0.94	DWS	1.0 ± 0.1	50 ± 5	15 ± 2	37 ± 1	15.0 ± 0.5	43 ± 1	5.4 ± 0.2	48 ± 4	160 ± 50
1.47	OTI	1.0 ± 0.1	60 ± 6	30 ± 3	37 ± 1	15.0 ± 0.5	41 ± 1	5.2 ± 0.2	43 ± 3	90 ± 20
1.47	DWS	3.0 ± 0.1	60 ± 6	30 ± 3	25.7 ± 0.3	10.4 ± 0.1	41 ± 1	5.2 ± 0.2	69 ± 3	140 ± 40

experimental methods at higher frequencies. Equation (1) applied to the inertia-corrected MSDs and to the Indei-Schieber method [Eq. (2)] yield to similar results, matching the theoretical curves and the $\omega^{3/4}$ behavior, especially when using OTI and small beads. Differences between both methods arise when using DWS and bigger beads, where Eq. (2) provides better results.

In conclusion, our experimental data and analysis demonstrate that, when properly accounting for inertia effects, passive microrheology easily provides access to the mechanical properties of viscoelastic fluids up to frequencies in the MHz scale. The correction procedure is simplified by the availability of an analytical expression that can be applied straightforwardly to the experimental data. This procedure extends the range of application of microrheology up to two orders of magnitude, and therefore will enable new experiments in a regime which is fairly inaccessible to traditional mechanical rheometry.

We acknowledge B. U. Felderhof and T. Franosch for helpful discussions. P.D.G acknowledges M.E.C.D. for financial aid by Plan Nacional I+D+i 2008-2011 and project FIS2013-47350-C5-5-R. P.D.G. and S.J. acknowledge support from the NCCR-Nano (project 1.4). F.S. acknowledges financial support by the Swiss National Science Foundation under Grants No. 132736 and No. 149867.

[1] A. Einstein, Ann. Phys. **17**, 549 (1905).
[2] T. G. Mason and D. A. Weitz, Phys. Rev. Lett. **74**, 1250 (1995).
[3] T. A. Waigh, Rep. Prog. Phys. **68**, 685 (2005).
[4] A. Einstein, Ann. Phys. **19**, 371 (1906).
[5] T. Franosch, M. Grimm, M. Belushkin, F. M. Mor, G. Foffi, L. Forró, and S. Jeney, Nature (London) **478**, 85 (2011).
[6] T. Li and M. Raizen, Ann. Phys. **525**, 281 (2013).
[7] T. B. Liverpool and F. C. MacKintosh, Phys. Rev. Lett. **95**, 208303 (2005).
[8] M. Atakhorrami, D. Mizuno, G. H. Koenderink, T. B. Liverpool, F. C. MacKintosh, and C. F. Schmidt, Phys. Rev. E **77**, 061508 (2008).
[9] B. Fabry, G. N. Maksym, J. P. Butler, M. Glogauer, D. Navajas, and J. J. Fredberg, Phys. Rev. Lett. **87**, 148102 (2001).
[10] C. Oelschlaeger, M. Cota Pinto Coelho, and N. Willenbacher, Biomacromolecules **14**, 3689 (2013).
[11] D. C. Vadillo, T. R. Tuladhar, A. Mulji, and M. R. Mackley, J. Rheol. **54**, 781 (2010).
[12] M. L. Gardel, M. T. Valentine, J. C. Crocker, A. R. Bausch, and D. A. Weitz, Phys. Rev. Lett. **91**, 158302 (2003).
[13] N. Willenbacher, C. Oelschlaeger, M. Schopferer, P. Fischer, F. Cardinaux, and F. Scheffold, Phys. Rev. Lett. **99**, 068302 (2007).
[14] T. Indei, J. D. Schieber, and A. Córdoba, Phys. Rev. E **85**, 041504 (2012).
[15] A. Córdoba, T. Indei, and J. D. Schieber, J. Rheol. **56**, 185 (2012).
[16] F. Gittes and F. C. MacKintosh, Phys. Rev. E **58**, R1241 (1998).
[17] A. J. Levine and T. C. Lubensky, Phys. Rev. Lett. **85**, 1774 (2000).
[18] S. Jeney, F. Mor, R. Koszali, L. Forró, and V. T. Moy, Nanotechnology **21**, 255102 (2010).
[19] A. Ashkin, Science **210**, 1081 (1980).
[20] G. Maret and P.-E. Wolf, Z. Phys. B: Condens. Matter **65**, 409 (1987).
[21] D. J. Pine, D. A. Weitz, P. M. Chaikin, and E. Herbolzheimer, Phys. Rev. Lett. **60**, 1134 (1988).
[22] T. G. Mason, K. Ganesan, J. H. van Zanten, D. Wirtz, and S. C. Kuo, Phys. Rev. Lett. **79**, 3282 (1997).
[23] M. T. Valentine, Z. E. Perlman, M. L. Gardel, J. H. Shin, and P. Matsudaira, Biophys. J. **86**, 4004 (2004).
[24] M. Cates and S. Candau, J. Phys.: Condens. Matter **2**, 6869 (1990).
[25] M. Buchanan, M. Atakhorrami, J. F. Palierne, F. C. MacKintosh, and C. F. Schmidt, Phys. Rev. E **72**, 011504 (2005).
[26] M. Grimm, T. Franosch, and S. Jeney, Phys. Rev. E **86**, 021912 (2012).
[27] Calibration values for Fig. 1 are $\beta = 10.3\ \mu$m/V for $a = 0.94\ \mu$m and $\beta = 19.9\ \mu$m/V for $a = 1.47\ \mu$m.
[28] P. Zakharov, F. Cardinaux, and F. Scheffold, Phys. Rev. E **73**, 011413 (2006).
[29] F. Cardinaux, L. Cipelletti, F. Scheffold, and P. Schurtenberger, Europhys. Lett. **57**, 738 (2002).
[30] C. Oelschlaeger, M. Schopferer, F. Scheffold, and N. Willenbacher, Langmuir **25**, 716 (2008).
[31] D. T. Chen, E. R. Weeks, J. C. Crocker, M. F. Islam, R. Verma, J. Gruber, A. J. Levine, T. C. Lubensky, and A. G. Yodh, Phys. Rev. Lett. **90**, 108301 (2003).
[32] S. Chandrasekhar, Rev. Mod. Phys. **15**, 1 (1943).
[33] E. Hinch, J. Fluid Mech. **72**, 499 (1975).
[34] T. G. Mason, Rheol. Acta **39**, 371 (2000).
[35] R. M. L. Evans, M. Tassieri, D. Auhl, and T. A. Waigh, Phys. Rev. E **80**, 012501 (2009).
[36] See Supplemental Material at http://link.aps.org/supplemental/10.1103/PhysRevE.90.060301 for a comparison of the two methodologies using our data.
[37] T. D. Squires and T. G. Mason, Annu. Rev. Fluid Mech. **42**, 413 (2010).
[38] E. J. G. Peterman, M. A. van Dijk, L. C. Kapitein, and C. F. Schmidt, Rev. Sci. Instrum. **74**, 3246 (2003).
[39] K. Berg-Sørensen and H. Flyvbjerg, Rev. Sci. Instrum. **75**, 594 (2004).
[40] D. Mizuno, D. A. Head, F. C. MacKintosh, and C. F. Schmidt, Macromolecules **41**, 7194 (2008).
[41] In that work, the Fourier transform was carried out first on the measured time series of bead positions to obtain the PSD. The inertia correction is then executed on the PSD using the known expression for the frequency dependent particle mobility in a simple liquid using an effective complex viscosity of the medium derived from the experimental data.
[42] B. U. Felderhof, J. Chem. Phys. **131**, 164904 (2009).
[43] Equation (37) of Ref. [14] is the following: $G^*(\omega) = \frac{k_B T}{i\omega\pi a\overline{\mathrm{MSD}}} + \frac{m^*\omega^2}{6\pi a} + \frac{a^2\omega^2}{2}[\sqrt{\rho^2 + \frac{2\rho}{3\pi a^3}(\frac{6k_BT}{(i\omega^3\overline{\mathrm{MSD}})} - m^*)} - \rho]$, which can be related to Eq. (1) since the term in the square root is $6k_BT/(i\omega^3\overline{\mathrm{MSD}}) = -(6\pi a/\omega^2)\, Z^*(\omega)$.

[44] An equivalent figure for $a = 1.47\mu$m is included in the Supplemental Material [36] .
[45] Using the GSER at high frequencies can introduce nonexpected effects. See the Supplemental Material [36] document for extra comments about this point.
[46] M. Doi and S. F. Edwards, *The Theory of Polymer Dynamics* (Clarendon Press, Oxford, 1986).
[47] For DWS experiments we use G_0 and G''_{min} from OTI. We select ω_0 for the experimental G^* to match G^*_{GMK}, obtaining $\omega_0 \sim 10^4$Hz, consistent with literature values .